SENSORLESS SLIDING MODE CONTROL OF MAGNETIC BEARING ACTUATORS USING IMPLICIT SWITCHING SURFACES

Lichuan Li
Dept. of Mechanical Engineering, Xi'an Jiaotong University, Xi'an, China, lcli@xjtu.edu.cn
Paul E. Allaire
MANE Department, University of Virginia, Charlottesville, VA, USA, pea@virginia.edu

ABSTRACT
Sensorless sliding mode control of a single-axis pull-pull type magnetic bearing actuator is reported in this paper. The two electromagnets are driven by switching between a positive and a negative constant voltage. Two switching surfaces being indirectly available through the measurement of driving current and its change rate are constructed, but only one of which is available at any time. Sliding mode control using these two switching surfaces in turn is shown to be possible. Reaching condition and the stability of sliding dynamics are discussed. The sliding mode turns out to take place in a subregion of state space defined by $s_1(\boldsymbol{x})s_2(\boldsymbol{x})\leq 0$ rather than on a surface defined by $s(\boldsymbol{x})=0$ as in most standard cases. The mathematical results are verified by simulation and experiment.

INTRODUCTION
Sensorless and self-sensing control of magnetic bearings, though the resultant precision is lower than with sensors, are appealing for some applications due to hardware simplicity and cost-effectiveness. When the electromagnets are being driven by either voltage or current, the relationship between voltage and current takes the information of displacement and velocity. This provides a possibility of stabilization and control without using explicit displacement sensors. This approach is grouped into two categories [3]: sensorless and self-sensing. In the former case there is no direct effort of displacement information extraction and observers are mostly used, while in the latter case displacement is explicitly calculated.

For the sake of power effectiveness, switching power amplifiers are being widely used in magnetic bearings. In this case the electromagnets are switched between a positive and a negative constant voltage. This switching driving readily provides an environment for the implementation of sliding mode control. What is more, under such switching driving, some scalar functions of state variables are available through the measurement of current and its change rate, both being easier than the measurement of displacement. Using surfaces defined by these functions, sliding mode control may be possible without any displacement sensor. This paper explores this possibility and some of the associated problems.

Both sensorless/self-sensing and sliding mode control have been active topics in magnetic bearing research. Sensorless control using Luenberger state observers is presented as a nice application example of the well established linear systems theory [1]-[2]. Various kinds of self-sensing have also been reported. Displacement is estimated using a reference model that runs in real-time [3], or by the driving frequency under a hysteresis power amplifier [4], or by superposing a high-frequency sinusoidal current on the driving current [5]. Reports on sliding mode control of magnetic bearings are also found in the literatures. A discrete-time sliding mode controller is designed for a magnetic bearing for improving the robustness [6]. A sliding mode controller is used with a sliding mode observer for enhancing the stabilization and tracking performance [7]. Sliding mode control design equations dealing with various uncertainties are developed based on a magnetic bearing example [8]. Attention has also been paid to sliding mode control with integral compensation for achieving zero steady-state error [9]. This paper is more of sensorless control. Sliding mode control comes only as utilization of available equations under switching driving and switching driving itself. But it gives new facts in both sensorless and sliding mode control.

MAGNETIC BEARING ACTUATOR
A single-axis magnetic bearing actuator as shown in Fig. 1 is considered. A photograph of such a physical object is found in Fig. 3. In this section the equations of this object is given, which provides a basis for subsequent discussions.

In Fig. 1, the motion of the ferromagnetic moving object, which is of mass m, is limited in the x-axis only. The voltages u_1 and u_2 are taken as the input of the

plant. The external resistors of resistance R denote copper resistance of the coils and may include possible current-sampling resistors. It is assumed that the permeability of the magnetic material is constant, and the flux density over the air gap is uniformly distributed. It is also assumed that the effects of eddy current, flux stray and flux leakage are small. We ignore such effects in this paper. Then, the equations of the plant are [10]

$$m\ddot{x} = \frac{1}{\mu_0 A}\left(\phi_2^2 - \phi_1^2\right) + f_d \tag{1a}$$

$$N\dot{\phi}_1 + Ri_1 = u_1, \quad N\dot{\phi}_2 + Ri_2 = u_2 \tag{1b}$$

$$i_1 = \frac{2}{\mu_0 AN}(x_0 + x)\phi_1, \quad i_2 = \frac{2}{\mu_0 AN}(x_0 - x)\phi_2 \tag{1c}$$

where x_0=g+l, l accounts for the effect of the finiteness of permeability, f_d is the disturbance force, ϕ_1 and ϕ_2 are fluxes due to i_1 and i_2 respectively, and A is the electromagnet pole face area. These equations, except for some minor differences, are also found in many literatures on magnetic bearings.

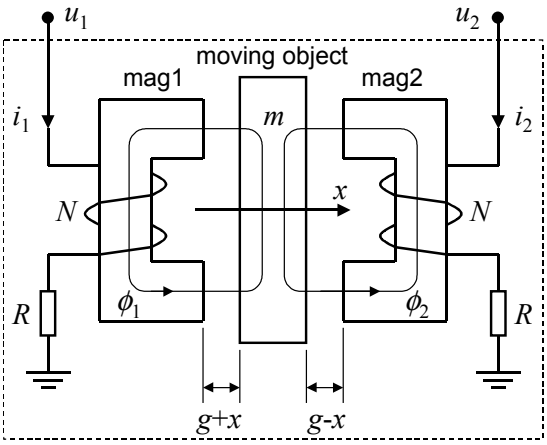

FIGURE 1: Schematic of Actuator

For succinctness in following discussions, let (1) be in normalized variables. Choosing a nominal biasing current I_0, the variables are normalized as ξ=x/x_0, η_1=i_1/I_0, η_2=i_2/I_0, θ=f_d/mx_0, ε_1=u_1/RI_0, ε_2=u_2/RI_0, ψ_1=ϕ_1/Φ_0 and ψ_2=ϕ_2/Φ_0, where Φ_0=$\mu_0 ANI_0/2x_0$ is the nominal biasing flux. With the normalized variables (1) becomes

$$\ddot{\xi} = \alpha\left(\psi_2^2 - \psi_1^2\right) + \theta \tag{2a}$$

$$\frac{1}{\beta}\dot{\psi}_1 + \eta_1 = \varepsilon_1, \quad \frac{1}{\beta}\dot{\psi}_2 + \eta_2 = \varepsilon_2 \tag{2b}$$

$$\eta_1 = (1+\xi)\psi_1, \quad \eta_2 = (1-\xi)\psi_2 \tag{2c}$$

where α=$\mu_0 AN^2 I_0^2/4mx_0^3$ and β=$2Rx_0/\mu_0 AN^2$. Concept about reasonable orders of the normalized variables is useful in subsequent sections. It is seen that $|\xi|<1$, ψ's and η's are both on the order of 1, and maximum possible values of ε's are on the order of 10 (probably greater than ten due to the requirement of a sufficient force slew rate). For most practical systems α and β are on the orders of 10^4 and 10^2 respectively.

SENSORLESS SLIDING MODE CONTROL

It is assumed that the internal of the dashed block in Fig. 1 is not accessible. We have only available the coil terminals for control. This may be an appropriate situation we face for sensorless control. We search, starting from (2), for equalities that at one side the quantity is useful for control while at the other side the quantity is readily or easily measured outside the dashed block. Rearranging (2c) with the term $\xi\psi$'s alone on the left-hand side, we have

$$\xi\psi_1 = \eta_1 - \psi_1, \quad \xi\psi_2 = -\eta_2 + \psi_2 \tag{3}$$

Then, differentiating (3) with respect of time yields

$$\psi_1\dot{\xi} + \dot{\psi}_1\xi = \dot{\eta}_1 - \dot{\psi}_1 = \dot{\eta}_1 - \beta(\varepsilon_1 - \eta_1) \tag{4a}$$

$$\psi_2\dot{\xi} + \dot{\psi}_2\xi = -\dot{\eta}_2 + \dot{\psi}_2 = -\dot{\eta}_2 + \beta(\varepsilon_2 - \eta_2) \tag{4b}$$

It is seen that the left-hand sides of (4) are linear in displacement and velocity, and may serve as part of switching functions for sliding mode control (the other part is acceleration, as under voltage control the plant is of third-order). Besides, the variables on the right-hand sides are easily measured: current and its change rate are measured by connecting sampling resistors and inductors in series with the coils, both being outside the dashed block. However, as coefficients the fluxes and their change rates are not of constant values. This may cause problem. Even worse is that flux change rate cannot have a single sign all the time.

If driving current is limited to be unidirectional, then ψ_1 and ψ_2 can be nonnegative. If further a substantial biasing current is maintained, then the fluxes can be positive and relatively stable. Besides, if switching driving is used, which is in consistent with sliding mode control, then problems associated with the flux change may be relieved. Let the input voltages be switched between constant positive and negative voltages, that is,

$$\varepsilon_1 = 1 - (U/RI_0)\mu, \quad \varepsilon_2 = 1 + (U/RI_0)\mu \tag{5}$$

where U is a positive physical voltage, and $\mu \in \{-1, 1\}$ is a new control input. This is the constant voltage sum (CVS) configuration for maintaining the nominal biasing current I_0 [10]. Note that (5) implies ε_1+ε_2=2. The physical driving voltages are switched between RI_0+U and RI_0-U. If U/RI_0 is much greater than 1, then

between consecutive switching instants, $d\psi_1/dt$ and $d\psi_2/dt$ are close to some constants, since in (2b) compared with ε's the values of η's are much smaller. It is also noticed that the orders of $\{\psi_1, \psi_2\}$ and $\{d\psi_1/dt, d\psi_2/dt\}$ are 1 and 10^3 respectively, being desirable as coefficients of linear switching surfaces. Another fact to notice is that at any time either $d\psi_1/dt$ or $d\psi_2/dt$ has positive sign. This motivates an attempt of using equations (4a) and (4b) in turn, depending on the sign of μ, for sensorless sliding mode control.

Some effect of acceleration should be included in switching surfaces. To this end, (2c) is manipulated to yield

$$\psi_2 - \psi_1 = \eta_2 - \eta_1 + \xi(\psi_1 + \psi_2) \tag{6}$$

Substituting (6) into (2a) and assuming θ=0, we have

$$\ddot{\xi} = \alpha(\psi_1 + \psi_2)(\eta_2 - \eta_1) + \alpha\xi(\psi_1 + \psi_2)^2 \tag{7}$$

The flux sum $\psi_1+\psi_2$ is very close to 2 under CVS [12]. The second term on the right-hand side, which is linear in ξ, can be included in the displacement. Thus, $C(\eta_2-\eta_1)$, where C is a positive constant, may be used in switching surfaces for acceleration.

Now, the above mentioned facts are pieced together to formulate our possible switching functions as

$$s_1 = C(\eta_2 - \eta_1) + \psi_1\dot{\xi} + \dot{\psi}_1\xi \tag{8a}$$
$$s_2 = C(\eta_2 - \eta_1) + \psi_2\dot{\xi} + \dot{\psi}_2\xi \tag{8b}$$

Equations s_1=0 and s_2=0 are surfaces in the state space when μ is constant. It is obvious from (4) that the switching functions s_1 and s_2 can be evaluated by the measurement of η_1, η_2, $d\eta_1/dt$ and $d\eta_2/dt$. The coefficients in (8a) are all positive when μ=-1, and so are those in (8b) when μ=1. The attempted sliding mode control algorithm is thus constructed in discrete time as below.

At each sampling instant,
if $\mu = -1$ and $s_1 < 0$, **then** let $\mu = 1$, (9)
else if $s_2 > 0$, **then** let $\mu = -1$.

It is noted that a continuous time version of (9) is also possible, but in discrete time it is easier to describe. It is assumed that the sampling rate is very high that there is no significant difference between discrete and continuous time implementations. In fact, a sampling rate of 100 kHz is chosen for both simulation and experiment in this paper.

One may wonder whether this algorithm works. It was tested in simulation and it did work. Then mathematical explanations were found and experiment was carried out. But here in this paper the mathematical analysis is given ahead of simulation and experiment.

REACHING CONDITION

The switching functions s_1 and s_2 are directly related to the flux change rates, which are not state variables. In order to facilitate the analysis we give equivalent switching functions that are functions of state variables alone. Because s_1 is checked only when μ=-1 and s_2 is checked only when μ=1, these switching functions can be redefined as

$$s_1 = C(\eta_2 - \eta_1) + \psi_1\dot{\xi} + \beta(\rho - \eta_1)\xi \tag{10a}$$
$$s_2 = C(\eta_2 - \eta_1) + \psi_2\dot{\xi} + \beta(\rho - \eta_2)\xi \tag{10b}$$

without any influence on the algorithm (9), where $\rho=1+U/RI_0$ is the positive amplitude of the normalized voltage inputs. Hereafter s_1 and s_2 mean those defined in (10). It is not hard to see that under first-order approximation about the equilibrium point s_1 and s_2 become identical and are linear functions of $d^2\xi/dt^2$, $d\xi/dt$ and ξ. With the redefined switching functions, the previous problem that flux change rate cannot have a single sign all the time is now transformed as only one of the switching functions in (10) is available at any time through the measurement of driving current and its change rate, except for instants μ being switched between -1 and 1.

For the algorithm (9) to work a basic requirement is that the conditions for the if's can actually become satisfied. It is therefore required that $ds_1/dt<0$ when μ=-1 and $ds_2/dt>0$ when μ=1. But this is not enough. For the reasons to be clear below, it is also required that $ds_2/dt<0$ when μ=-1 and $ds_1/dt>0$ when μ=1. It is therefore assumed that $|d\xi/dt|$ is bounded and U is sufficiently high such that the following conditions hold.

$$\dot{s}_1 < 0,\ \dot{s}_2 < 0 \quad \text{when } \mu = -1 \tag{11a}$$
$$\dot{s}_1 > 0,\ \dot{s}_2 > 0 \quad \text{when } \mu = 1 \tag{11b}$$

It will be seen bellow that this is the reaching condition for the sliding mode control.

In standard sliding mode control, the number of switching surfaces is equal to that of control variables. But here there are two switching surfaces while there is only one control input. It is generally impossible to keep both s_1=0 and s_2=0. The algorithm (9) can at most maintain s_1 and s_2 close to zero. It actually tries to get out of the situation $s_1s_2>0$ in the reaching phase. Then, if the switching is infinitely fast, it maintains $s_1s_2\le 0$ in the sliding phase. Under infinitely fast switching, the running of the algorithm is more clearly seen: if $s_1<0$ and $s_2<0$, then μ=1 until s_2=0; if $s_1>0$ and $s_2>0$, then μ=-1 until s_1=0; if $s_1\le 0$ and $s_2\ge 0$, then μ is switched between -1 and 1 with 50% duty cycle; and if $s_1\ge 0$ and $s_2\le 0$, then μ is switched between -1 and 1 such that s_1

and s_2 just reach zero in turn. Thus, once $s_1 s_2 \le 0$ becomes true it will remain true in future time, and this indicates the entering of sliding mode. These switching laws are summarized in Fig. 2. It is not hard to notice that the reaching condition (11) must be true to guarantee the algorithm to run properly.

Unlike standard sliding mode control where sliding occurs on surfaces or in subspaces of the state space, here the sliding occurs in a subregion of the state space. One may also notice, as shown in Fig. 2, that the reaching behaviors in the two reaching regions are symmetrical while the sliding behaviors in the two sliding regions are not.

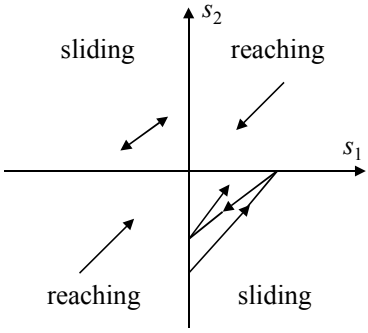

FIGURE 2: Reaching and Sliding Regions

STABILITY OF SLIDING DYNAMICS

In order for succinctness of equations, let $\psi_0=(\psi_1+\psi_2)/2$ and $\psi=(\psi_2-\psi_1)/2$, referred to as biasing and actuating flux respectively. Similarly, let $\eta_0=(\eta_1+\eta_2)/2$ and $\eta=(\eta_2-\eta_1)/2$, referred to as biasing and actuating current respectively. Note that at equilibrium we have $\psi_0=\eta_0=1$. From (2c) we also have

$$\eta_0 = \psi_0 - \xi\psi \qquad (12)$$
$$\eta = \psi - \xi\psi_0 \qquad (13)$$

Let $s_0=(s_1+s_2)/2$. Then it follows from (10) and (12)-(13) that

$$\frac{2C+\beta\xi^2}{4\alpha\psi_0}\ddot{\xi} + \psi_0\dot{\xi} + [\beta\rho - (2C+\beta)\psi_0]\xi = s_0 \qquad (14)$$

Adding the two equations in (2b) and substituting (5) and (12)-(13), we arrive at

$$\frac{1}{\beta}\dot{\psi}_0 + \psi_0 = 1 + \xi\psi \qquad (15)$$

Equations (14)-(15) are looked upon as state equations of a 3th-order system with inputs on the right-hand sides. It is seen that if $s_0=0$ then the autonomous system is locally stable about the equilibrium point $\xi=d\xi/dt=0$ and $\psi_0=1$. Since in sliding mode $s_1 s_2 \le 0$ is true, which implies $|s_1+s_2| \le |s_2-s_1|$, that is

$$|s_0| \le \left|\psi\dot{\xi} - \beta\psi\xi + \beta\psi_0\xi^2\right| \qquad (16)$$

Thus s_0 is bounded by a quadratic function of the states and the sliding dynamics is locally stable. It is noted that though the system (14)-(15) is of 3rd-order, the sliding dynamics is of 4th-order. As (16) is an inequality, s_0 is not a function of the state variables ξ, $d\xi/dt$ and ψ_0. Thus $d^2\xi/dt^2$ in (14) is not a function of the state variables but a fourth state variable. The sliding dynamics is not completely determined by the switching surfaces. Even if the reaching condition (11) is true, the robustness associated with standard sliding mode control is lost.

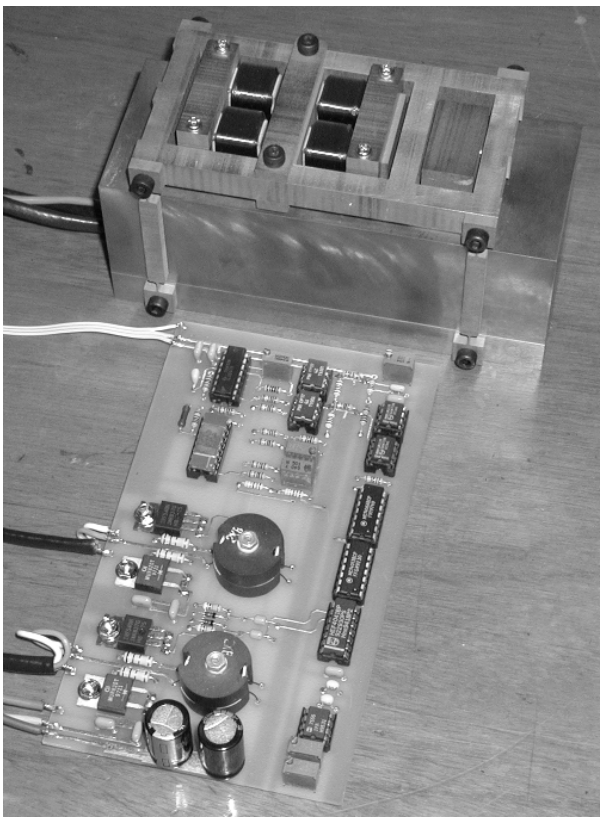

FIGURE 3: Experimental Actuator and Electronics

SIMULATION AND EXPERIMENT

A photo of the experimental actuator and electronics is given in Fig. 3. The parameters of the actuator are $A=10^{-4}$ m^2, $N=324$, $m=0.324$ kg, $x_0=0.35\times10^{-3}$ m and $R=0.27\ \Omega$ which includes a 0.5 Ω current-sampling resistance. The effect of the finiteness of permeability is not considered, that is, $l=0$. For other parameters,

I_0=0.8 A, U=25 V and C=300 are chosen. Transformers of 1:1 with an inductance of 1×10^{-4} H in both sides are used for the measurement of current change rate. The sampling rate is 100 kHz. In simulation the same parameters are used. Both simulation and experiment are done first using (10) and then with a term z as determined by

$$\tau\dot{z} + z = -C(\eta_2 - \eta_1) \qquad (17)$$

being added to the right-hand sides of (10a) and (10b), thus canceling the term $C(\eta_2$-$\eta_1)$ under steady-state. The value of τ is 5×10^{-3} s. This is the familiar concept of disturbance observation for achieving zero steady-state error under external disturbance force θ.

Simulation results of startup from ξ=-0.9, with other initial states being zero, are shown in Fig. 4. It is assumed that the motion axis is vertical, so that the mass of the moving part causes a static displacement in Fig. 4a. Experimental results are shown in Fig. 5. It is started by switching on the power from ξ=-1. Obvious differences are seen between Fig. 5a-b and Fig. 4a-b. In the experiment, apart from longer transient, the static stiffness is much lower. These differences are not further investigated. Fig. 5c-d show the response to a sudden removal of a load of 3.332 N at the time of 50 ms.

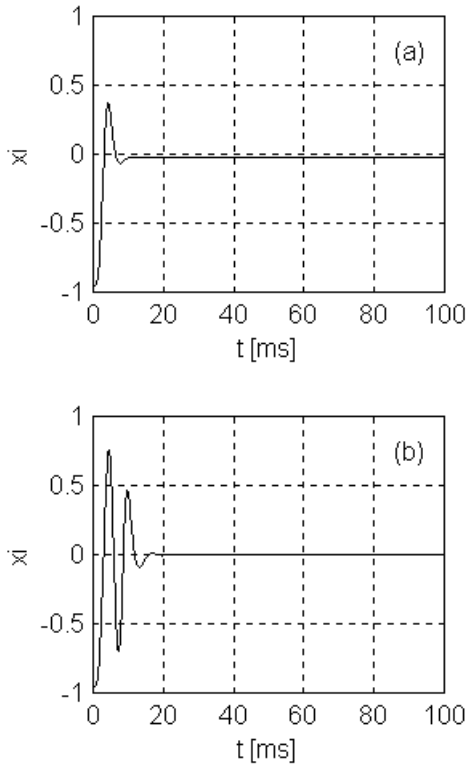

FIGURE 4: Simulation Results
(a) startup without disturbance observer, (b) startup with disturbance observer

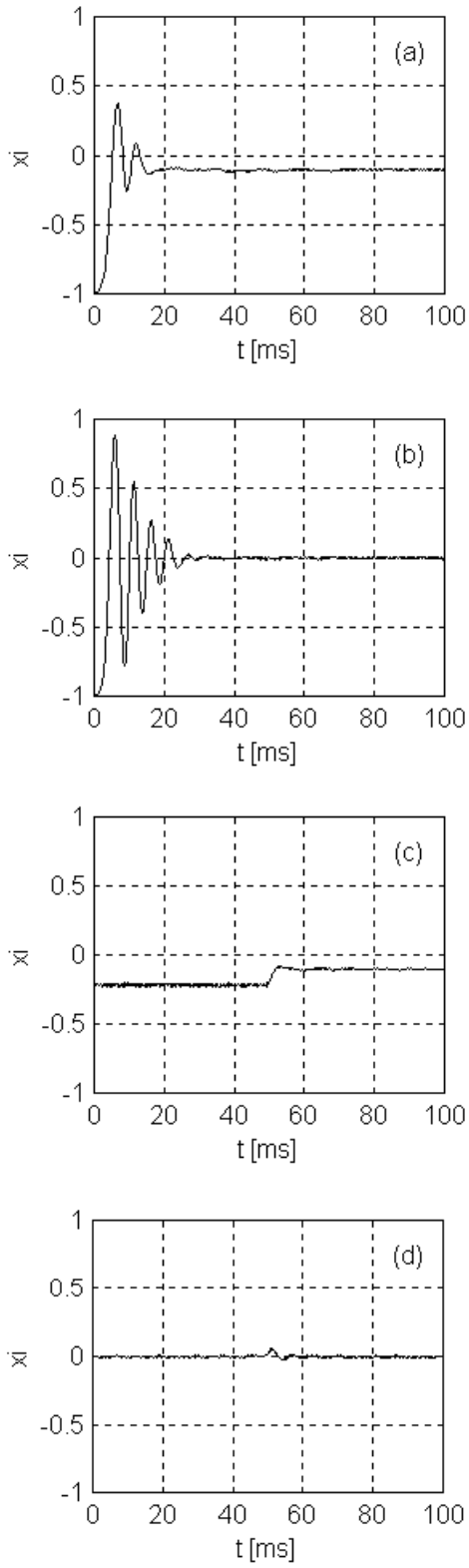

FIGURE 5: Experiment Results
(a) startup without disturbance observer, (b) startup with disturbance observer, (c) sudden removal of load without disturbance observer, (d) sudden removal of load with disturbance observer

It is observed in both simulation and experiment that performance is sensitive to some of the parameters and the symmetry of the two sides. The switching function values are close to zero under steady-state. But they are based on the canceling of two large values: the two terms on the right-hand sides of (4). A small percentage error on β used for the construction of the right-hand sides of (4) will cause large errors of s_1 and s_2 when the state is close to the equilibrium point. As a result, if β is not matched with the real value, then either the actual switching frequency becomes much lower than 100 kHz, or the equilibrium displacement splits into two on both sides of ξ=0. There is also considerable noise in the displacement, as can be seen in Fig. 5. The noise comes chiefly from the measurement of current change rate.

CONCLUSIONS

Under switching driving, as the input voltages are piecewise constant, some functions of state variables are available through the measurement of driving current and its change rate. Using these functions as switching functions, the system state is conducted towards and then kept in a subregion of the state space, in which the system dynamics is stable. Thus sensorless control is realized at the measurement of driving current and its change rate.

Sliding mode control is employed for magnetic bearings for the associated robustness. In this paper, however, sliding mode control is used due to the very format of the available information under switching driving. As a result, two switching surfaces are used in turn and the state is only kept within a subregion other than a subspace. Thus the good properties of sliding mode control are lost. The sliding dynamics is dependent on disturbance and plant parameters such as biasing current and amplitude of driving voltage. The noise in the experiment is also a problem. Further investigation may include the avoidance of these problems.

REFERENCES

1. D. Vischer and H. Bleuler, A New Approach to Sensorless and Voltage Controlled AMBs Based on Network Theory Concepts, *Proc. 2nd Int. Symp. Magnetic Bearings*, July 12-14, 1990, Tokyo, Japan, pp. 301-306

2. T. Shinshi, K. Sato and A. Shimokohbe, Precision Sensorless Positioning of Magnetic Levitation System, *Proc. 9th Int. Precision Engineering Seminar and 4th Int. Conf. on Ultraprecision in Manufacturing Engineering*, May 26-30, 1997, Braunschweig, Germany, vol. 2, pp. 492-494

3. M. D. Noh and E. H. Maslen, Self-Sensing Magnetic Bearings Using Parameter Estimation, *IEEE Trans. Instrum. Meas.*, vol. 46, no. 1, February 1997, pp. 45-50

4. T. Mizuno, H. Namiki and K. Araki, Counter-Interfaced Digital Control of Self-Sensing Magnetic Suspension Systems with Hysteresis Amplifiers, *JSME Int. J. Series C*, vol. 42, no. 1, March 1999, pp. 71-78

5. V. M. G. van Acht, A. A. H. Damen and P. P. J. van den Bosch, On Self-Sensing Magnetic Levitated Systems, *Proc. 6th Int. Symp. Magnetic Bearings*, August 5-7, 1998, MIT, MA, USA, pp. 538-547

6. H. Tian and K. Nonami, Robust Control of Flexible Rotor-Magnetic Bearing Systems Using Discrete Time Sliding Mode Control, *JSME Int. J. Series C*, vol. 37, no. 3, September 1994, pp. 504-512

7. A. E. Rundell, S. V. Drakunov and R. A. DeCarlo, Sliding Mode Observer and Controller for Stabilization of Rotational Motion of a Vertical Shaft Magnetic Bearing, *IEEE Trans. Contr. Syst. Tech.*, vol. 4, no. 5, September 1996, pp. 598-608

8. P. E. Allaire and A. Sinha, Robust Sliding Mode Control of a Planar Rigid Rotor System on Magnetic Bearings, *Proc. 6th Int. Symp. Magnetic Bearings*, August 5-7, 1998, MIT, MA, USA, pp. 577-586

9. Jun-Ho Lee, Edgar F. Hilton, Xuerui Zhang, Gang Tao and Paul E. Allaire, Integral Sliding Mode Controller for Magnetically Suspended Balance Beam: Theory and Experimental Evaluation, *Proc. 5th Int. Symp. Magnetic Suspension Technology*, Santa Barbara, CA, USA, December 1-3, 1999

10. L. Li, Linearizing Magnetic Bearing Actuators by Constant Current Sum, Constant Voltage Sum, and Constant Flux Sum, *IEEE Trans. Magnetics*, vol. 35, no. 1, January 1999, pp. 528-535